DMD #9514

Drug Metab. Dispos.

DIFFERENTIAL EFFECTS OF THE OXIDIZED METABOLITES OF OLTIPRAZ ON THE ACTIVATION OF C/EBPβ AND NRF2 FOR *GSTA2* GENE INDUCTION

MYONG SUK KO, SEUNG JIN LEE, JIN WAN KIM, JEE WOONG LIM AND SANG GEON KIM

National Research Laboratory, College of Pharmacy and Research Institute of Pharmaceutical Sciences, Seoul National University, Seoul 151-742, Korea (M.S.K.; S.J.L.; S.G.K.)

CJ Pharmaceutical Research Institute, CJ Corp., Kyonggi-Do, Korea (J.W.K; J.W.L.)

Running title: Effects of oltipraz's metabolites on C/EBPβ and Nrf2

Correspondence to: Sang Geon Kim, Ph.D., College of Pharmacy, Seoul National University, Sillim-dong, Kwanak-gu, Seoul 151-742, Korea. Tel: +822-880-7840; Fax: +822-872-1795; E-mail: sgk@snu.ac.kr

Number of figures: 7

Number of text pages: 25

Number of reference: 37

Number of words in Abstract: 250

Number of words in Introduction: 628

Number of words in Discussion: 1,655

ABBREVIATIONS: ARE, antioxidant response element; AUC, total area under the plasma concentration-time curve from time zero to time infinity; C/EBP, CCAAT/enhancer binding protein; C_{max}, peak plasma concentration; GST, glutathione S-transferase; MTT, [3-(4,5-dimethylthiazol-2-yl)-2,5-diphenyl-tetrazolium bromide]; Nrf2, NF-E2-related factor-2; NQO1, NAD(P)H:quinone oxidoreductase-1; PCR, polymerase chain reaction; SDS, sodium dodecylsulfate

ABSTRACT:

Comprehensive mechanistic studies suggest that oltipraz exerts cancer chemopreventive effects through the induction of glutathione S-transferase (GST). Previously, we have shown that the activation of CCAAT/enhancer binding protein-β (C/EBPβ), promoted by oltipraz, contributes to the transcriptional induction of the *GSTA2* gene. Studies also indicated that exposure of animals to oltipraz triggers nuclear accumulation of NF-E2-related factor-2 (Nrf2) with increase in Nrf2's antioxidant response element (ARE) binding activity. Given the previous reports that C/EBPβ activation contributes to oltipraz's induction of the *GSTA2* gene and that Nrf2 activation by oltipraz was variable depending on the concentrations, this study investigated whether the major oxidized metabolites of oltipraz induce GSTA2 through the activation of C/EBPβ and/or Nrf2. Immunoblot analysis revealed that M1 (4-methyl-5-(pyrazin-2-yl)-3H-1,2-dithiol-3-one) and M2 (7-methyl-6,8-bis(methylthio)H-pyrrolo[1,2-a]pyrazine), but not M3 and M4, induced GSTA2 in H4IIE cells. M1 and M2 also increased the luciferase activity from pGL-1651 which contained the luciferase structural gene downstream of the –1.65 kb GSTA2 promoter region. Nuclear C/EBPβ levels were enhanced by the metabolites, but not by M3 or M4. Among the oxidized metabolites examined, only M2, which elicited cell death at a relatively high concentration, activated Nrf2 as indicated by nuclear accumulation of Nrf2 and its ARE binding activity. The present study provides evidence that M1 and M2, but not M3 and M4, induce GSTA2 and that M1 induces GSTA2 only via C/EBPβ activation, while M2 does so by activating Nrf2 as well as C/EBPβ. These results substantiate the differential effects of oltipraz's metabolites on C/EBPβ- and/or Nrf2-mediated GSTA2 induction.

Oltipraz [4-methyl-5-(2-pyrazinyl)-1,2-dithiol-3-thione] has been studied as a chemopreventive agent for malignancies, such as liver and colorectal cancer (Kensler, 1997; Rao et al., 1993). Comprehensive mechanistic studies indicate that oltipraz exerts cancer chemopreventive effects through the induction of glutathione S-transferases (GSTs)(Kensler, 1997; Bolton et al., 1993). GST induction also accounts for the cytoprotective effect of oltipraz against toxicant-induced injury (Jaitovitch-Groisman et al., 2000; Nelson et al., 2002). A phase IIa randomized chemoprevention trial of oltipraz in residents of Qidong, China, showed that oltipraz might be clinically active as a chemopreventive agent. In the human studies, oltipraz dosage regimens with higher doses and long-dosing interval seemed to be more efficacious in preventing cancer, as supported by significant decline in the levels of aflatoxin-albumin adduct in the individuals receiving a higher dose of oltipraz (500 mg/week)(Wang et al., 1999; Jackson and Groopman, 1999; Jacobson et al., 1997).

Exposure of experimental animals to oltipraz triggers nuclear accumulation of NF-E2-related factor-2 (Nrf2)(Iida et al., 2004; Ramos-Gomez et al., 2001) and enhances Nrf2's antioxidant response element (ARE) binding activity (Pietsch et al., 2003). Diminished expression of phase II enzyme genes by oltipraz in the Nrf2$^{(-/-)}$ mice supported the role of Nrf2 activation in its cancer chemopreventive effects (Kwak et al., 2001; Ramos-Gomez et al., 2001). Molecular signals activated by oxidative stress stimulate translocation of Nrf2 to the nucleus, where it binds and activates the AREs located in the promoter regions of phase II enzyme genes (Venugopal and Jaiswal, 1998; Moinova and Mulcahy, 1998; Huang et al., 2000).

Studies from this laboratory showed that oltipraz at clinically relevant concentrations marginally increased the band intensity of Nrf2 ARE binding, and thus weakly enhanced the accumulation of Nrf2 in the nucleus. Our results suggested that GSTA2 induction by oltipraz might be mediated by the activation of other transcriptional factor(s) besides Nrf2. We have shown that oltipraz activates CCAAT/enhancer binding protein-β (C/EBPβ), which enhances the induction of the *GSTA2* gene via C/EBPβ DNA binding in the gene promoter (Kang et al., 2003). On the other hand, studies from other laboratories indicated that oltipraz treatment at higher concentrations (e.g., 70 μM, 500 mg/kg body weight) exhibited strong Nrf2 activation (Pietsch et al., 2003; Ramos-Gomez et al., 2001).

Because of the high lipid solubility of oltipraz, pharmacokinetics of oltipraz showed a tendency towards accumulation in organs, especially liver and large intestine (Bae et al., 2004). Hence, it is likely that oltipraz at high concentrations stays longer in the body, thereby increasing the production of its metabolites. It has been reported that oltipraz is metabolized by two major pathways in various mammalian species: (a) oltipraz is desulfurized and oxidized to yield M1, and M1 does not appear to be metabolized further; and (b) oltipraz may undergo a molecular rearrangement to yield M2, and then M2 is metabolized to other oxidized forms, M3 and M4 (O'Dwyer et al., 1997; Bieder et al., 1983). It has also been shown that M1 was active in inducing NAD(P)H:quinone oxidoreductase-1 (NQO1) in certain cells (O'Dwyer et al., 1997). Therefore, oltipraz's metabolites may also be active for the induction of phase II enzymes.

Given the previous findings that the activation of C/EBPβ contributed to the transcriptional induction of the *GSTA2* gene by oltipraz and that the activation of Nrf2 by oltipraz was variable depending on the concentrations, we were tempted to determine whether the oxidized metabolites of oltipraz play a role in the activation of C/EBPβ and/or Nrf2. This study investigated whether the major oxidized metabolites of oltipraz induce GSTA2 with the activation of C/EBPβ or Nrf2 and, if so, the efficacy of C/EBPβ or Nrf2 activation by the metabolites differs from that by the parent compound. Here, we report that the metabolites of oltipraz exert differential effects on the transcription factor activation for GSTA2 induction.

Materials and Methods

Materials. [γ-^{32}P]ATP (3000 mCi/mmol) was purchased from New England Nuclear (Arlington

Heights, IL). Anti-C/EBPβ and anti-Nrf2 antibodies were obtained from Santa Cruz Biotechnology

(Santa Cruz, CA). The antibodies specifically recognized their respective transcription factors without

any cross-reactivity. Horseradish peroxidase-conjugated goat anti-rabbit IgG was supplied from Zymed

Laboratories (San Francisco, CA).

Chemical Synthesis. Oltipraz and its metabolites (Fig. 1) were synthesized at the CJ Central

Laboratories (Ichon city, Korea) in the following procedures.

4-Methyl-5-(2-pyrazinyl)-1,2-dithiol-3-thione (Oltipraz): Methyl 2-methyl-3-(pyrazin-2-yl)-3-

oxopropionate (40 g, 206 mmole) dissolved in 100 ml of toluene was dropwise added to the mixture of

300 ml of toluene, 350 ml of xylene and 48 g (216 mmole) of phosphorous pentasulfide. Oltipraz

crystal obtained from chemical reaction of the mixture was filtered, washed and vacuum dried (6.37 g,

13.6% yield, >99.5%. purity). NMR(δ, CDCl$_3$): 2.51(s,3H), 8.70(d, 1H), 8.80(d, 1H), 9.21(s, 1H)

(Curphey, 2000; Curphey, 2002; Curphey and Libbyt, 2000)

4-Methyl-5-(pyrazin-2-yl)-3H-1,2-dithiol-3-one (M1): To a mixture of oltipraz (1.0 g, 4.42

mmole) in acetic acid (100 ml) and water (1.0 ml), mercuric acetate (1.97 g, 6.18 mmole) was added

portion-wise during 1.5 h. The suspended mixture was stirred at room temperature for 2 h. The

insoluble material was removed by filtration and washed with acetic acid, and the filtrate was poured

into water (500 ml). After extraction with ethyl acetate, organic phase was washed with water twice

and then with aqueous sodium bicarbonate. The solution was dried over anhydrous magnesium sulfate,

and evaporated *in vacuo*, and the residue was titrated with n-hexane to give red solid (0.3g, 32%). ^{1}H

NMR(400 MHz, CDCl$_3$) δ 2.40(s,3H), 8.70-8.75(m,2H), 9.05(s,1H). MS (EI) 210.1 (M$^+$)

7-Methyl-6,8-bis(methylthio)H-pyrrolo[1,2-a]pyrazine (M2): A mixture of oltipraz (2.5 g, 11.0

mmole), 0.01 M aqueous solution of ammonium acetate (350 ml), methanol (350 ml) and sodium

thiomethoxide (7.8 g, 111.3 mmole) was stirred at room temperature for 3 h. Iodomethane (5.3 ml,

85.1 mmole) was added to the solution, and stirred at room temperature for 3 h. After completing the

reaction, methanol was evaporated off. The mixture was extracted with ethyl acetate twice, and the

extract was washed with brine, dried over anhydrous sodium sulfate, and then evaporated. The residue was purified by chromatography on silica gel (ethyl acetate:n-hexane = 1:2) to yield yellowish solid (2.0 g, 81%). ^{1}H NMR(400 MHz, CDCl$_3$) δ 2.22(s,3H), 2.29(s,3H), 2.51(s,3H), 7.72(d,J=5.2Hz,1H), 8.22(d,J=1.4/5.2Hz,1H), 8.99(d,J=1.4Hz,1H). MS (FAB) 225.0 (M$^+$) (Corbet et al., 1982; Fleury et al., 1985; Largeron et al., 1987)

7-Methyl-8-(methylsulfinyl)-6-(methylthio)H-pyrrolo[1,2-a]pyrazine (M3): 7-Methyl-6,8-bis(methylthio)H-pyrrolo[1,2-a]pyrazine (0.5 g, 2.23 mmole) was dissolved in methylene chloride (10 ml) and the solution was cooled to –20°C. m-Chloroperoxybenzoic acid (1.0 g, 4.46 mmole, 77% assay) was added portion-wise to the reaction. The reaction solution was stirred at between –20°C and –15°C for 15 min, and then quenched with 1 M aqueous solution of potassium carbonate. The organic phase was retrieved and dried over anhydrous sodium sulfate. After evaporation, the residue was purified by chromatography on silica gel (ethyl acetate:methanol = 4:1) to yield white solid. ^{1}H NMR (400 MHz, CDCl$_3$) δ 2.23(s,3H), 2.59(s,3H), 3.01(s,3H), 7.85(d,J=5H,1H), 8.30(d,J=5Hz,1H), 9.33(s,1H). MS (FAB) 241.0 (M+1)

7-Methyl-6,8-bis(methylsulfinyl)H-pyrrolo[1,2-a]pyrazine (M4): This compound was prepared according to the same procedure, as described for the preparation of 7-methyl-8-(methylsulfinyl)-6-(methylthio)H-pyrrolo[1,2-a]pyrazine. Diastereomeric mixture; isomer 1: ^{1}H NMR (400 MHz, CDCl$_3$) δ 2.50(s,3H), 3.02(s,3H), 3.07(s,3H), 7.90(d,J=5.1Hz,1H), 8.78(dd,J=5.1Hz,1H), 9.43(s,1H); isomer 2: ^{1}H NMR (400 MHz, CDCl$_3$) δ 2.59(s,3H), 3.03(s,3H), 3.08(s,3H), 7.91(d,J=5.1Hz,1H), 8.82(dd,J=5.1Hz,1H), 9.57(s,1H). MS (FAB) 257.0 (M+1)

Cell Culture. H4IIE, a rat hepatocyte-derived cell line, was obtained from American Type Culture Collection (Rockville, MD). Cells were maintained in Dulbecco's modified Eagle's medium containing 10% fetal calf serum, 50 U/ml penicillin, and 50 μg/ml streptomycin at 37°C in a humidified atmosphere with 5% CO$_2$. Oltipraz or its metabolite, dissolved in dimethylsulfoxide, was added to the cells and incubated for the indicated time period for each experiment at 37°C. Cells were washed twice with ice-cold PBS before sample preparation.

Subcellular Fractionations. Total cell lysates and nuclear extracts were prepared according to

previously published methods (Ki et al., 2005). Briefly, H4IIE cells in dishes were washed twice with ice-cold PBS, scraped from the dishes with PBS and transferred to microtubes. To prepare cell lysates, the cells were centrifuged at 2,000g for 5 min and allowed to swell after the addition of the lysis buffer. The samples were centrifuged at 10,000g for 10 min to obtain lysates. To prepare nuclear extracts, the cells were centrifuged at 2,000g for 5 min and allowed to swell after the addition of 100 μl hypotonic buffer containing 10 mM HEPES (pH 7.9), 10 mM KCl, 0.1 mM EDTA, 0.5% Nonidet P-40, 1 mM dithiothreitol and 0.5 mM phenylmethylsulfonylfluoride. Lysate samples were incubated for 10 min on ice and then centrifuged at 7,200g for 6 min at 4°C. Pellets containing crude nuclei were resuspended in 50 μl of extraction buffer containing 20 mM HEPES (pH 7.9), 400 mM NaCl, 1 mM EDTA, 10 mM dithiothreitol, and 1 mM phenylmethylsulfonylfluoride, and then incubated for 30 min on ice. The samples were centrifuged at 15,800g for 10 min to obtain supernatants containing nuclear fractions. Nuclear fractions were stored at −70°C until use.

Immunoblot Analysis. SDS-polyacrylamide gel electrophoresis and immunoblot analysis were performed according to the previously published procedure (Ki et al., 2005). Briefly, protein samples were separated by 7.5% or 12% gel electrophoresis and electrophoretically transferred to nitrocellulose paper. The nitrocellulose paper was incubated with the antibody directed against GSTA2 (Detroit R&D, Detroit, MI), followed by incubation with a horseradish peroxidase-conjugated secondary antibody (Zymed Laboratories, San Francisco, CA). Specificity of the antibody to GSTA2 was previously determined (Kang et al., 2003). Immunoreactive protein was visualized by an ECL chemiluminescence detection kit (Amersham Biosciences, Buckinghamshire, UK). Equal loading of proteins was verified by Coomassie blue staining of gels and actin immunoblottings. At least three separate experiments were performed with different samples to confirm changes in the protein levels. Similarly, C/EBPβ or Nrf2 was immunochemically detected with their respective antibodies (Santa Cruz Biotechnology). Changes in the protein levels were determined via scanning densitometry of immunoblots using Image Scan & Analysis System (Alpha-Innotech Corp., San Leandro, CA). The area of each lane was integrated using the software AlphaEase version 5.5, followed by background subtraction.

[3-(4,5-Dimethylthiazol-2-yl)-2,5-diphenyl-tetrazolium bromide] (**MTT**) **Assay.** H4IIE cells

were plated at a density of 5×10^4 cells per well in a 96-well plate to determine cytotoxicity induced by each metabolite. Cells were serum-starved for 24 h, and exposed to the metabolite for 24 h at 37°C under 5% CO_2. After incubation of the cells, viable cells were stained with MTT (0.2 mg/ml, 3 h). The media were then removed and produced formazan crystals in the wells were dissolved by addition of 150 µl of dimethylsulfoxide. Absorbance was measured at 540 nm using a Titertek Multiskan Automatic ELISA microplate reader (Model MCC/340, Huntsville, AL). Cell viability was defined relative to control cells [i.e. viability (% control) = 100 × (absorbance of treated sample)/(absorbance of control)].

Gel Shift Assay. Double-stranded DNA probes containing C/EBP response element or ARE end-labeled with [γ-^{32}P]ATP, and T_4 polynucleotide kinase were used for gel shift analyses. Gel shift analyses for C/EBP and ARE bindings were carried out with the radiolabeled oligonucleotides 5'-TGCAGA<u>TTGCGCAA</u>TCTGCA-3' and 5'-GATCATGGCATTGCACTAGG<u>TGACAAAGCA</u>-3', respectively. The reaction mixture contained 4 µl of 5 × binding buffer [containing 50 mM Tris-HCl (pH 7.5), 20% glycerol, 5 mM MgCl$_2$, 250 mM NaCl, 2.5 mM EDTA, 2.5 mM dithiothreitol, and 0.25 mg/ml poly dI-dC], 10 µg of nuclear extract, and sterile water up to a total volume of 20 µl. The samples were preincubated without probe at room temperature for 10 min. The probe (1 µl, containing 10^6 cpm) was then added, and DNA-binding reactions were carried out for 30 min at room temperature. In some analyses, known as immuno-inhibition assays, antibodies directed to C/EBPα, C/EBPβ and Nrf2 (2 µg each) were added to the reaction mixture 20 min after the labeled probe was added, and the reaction was then continued for 1 h at 25°C. In other analyses, specificity of binding was determined by competition experiments, which were carried out by adding a 20-fold molar excess of an unlabeled C/EBP or ARE binding oligonucleotide to the reaction mixture before the labeled probe was added. SP-1 binding oligonucleotide (5'-ATTCGATCGGGGCGGGGCGAGC-3') was used as a negative control for competition experiments. Samples were separated on 4% polyacrylamide gels at 100 V. The gels were fixed with 40% methanol/10% acetic acid, dried, and subject to autoradiography.

GSTA2 Promoter-Luciferase Assay. The pGL-1651 reporter gene construct was generated by ligating the region 1.65 kb upstream of the transcription start site of the r*GSTA2* gene to the firefly luciferase reporter gene coding sequence, as described previously (Park et al., 2004; Lee and Kim,

2006). The mutants of GSTA2 promoter-luciferase plasmid, pGL-1651-ΔC/EBP and pGL-1651-ΔARE, in which the C/EBP response element and ARE were deleted, respectively, with the part of each sequence replaced with 5'-ctcgag-3', as described previously (Kang et al., 2003; Park et al., 2004; Lee and Kim, 2006). The studies using the mutants proved the functional role of the C/EBP response element and the ARE in the gene transactivation. To determine the activity of C/EBPβ- or ARE-mediated gene transactivation, we used the luciferase reporter assay system according to the published procedures (Park et al., 2004; Lee and Kim, 2006). Briefly, H4IIE cells (7×10^5 cells/well) were replated in six-well plates overnight, serum starved for 6 h, and transiently transfected with 1 μg of a promoter-luciferase construct and 0.3 μg of CMV-β-galactosidase plasmid (Invitrogen, Carlsbad, CA) in the presence of Lipofectamine Plus® Reagent for 3 h. Transfected cells were incubated in DMEM containing 1% fetal calf serum for 3 h and exposed to oltipraz or its metabolites (30 μM each) for 24 h at 37°C. For β-galactosidase activity, 10 μg of cell lysates was added to the solution containing 0.88 mg/ml o-nitrophenyl-β-D-galactopyranoside, 100 μM $MgCl_2$, and 47 mM β-mercaptoethanol in 100 mM sodium phosphate buffer. The reaction mixture was incubated for 12 h at 37°C and the absorbance was determined at 420 nm. The relative luciferase activity was calculated by normalizing firefly luciferase activity to that of β-galactosidase.

Statistical Analysis. One way analysis of variance (ANOVA) was used to assess statistical significance of differences among treatment groups. For each statistically significant effect of treatment, the Newman-Keuls test was used for comparisons between multiple group means. The data were expressed as means ±S.E. The criterion for statistical significance was set at $p < 0.05$ or $p < 0.01$.

Results

Effects of Oltipraz's Metabolites on GSTA2 Induction. First, we determined the expression of

GSTA2 after treatment of H4IIE cells with oltipraz, M1, M2, M3 or M4. Immunoblot analysis revealed

that treatment of cells with M1 (10-100 µM) for 24 h resulted in increases in the level of GSTA2 in a

concentration-dependent manner (Fig. 2A and 2B). The extent of GSTA2 induction by M1 at 30-100

µM was almost comparable to that by oltipraz. M2 (10-30 µM) also induced GSTA2. MTT assay

revealed that only M2 at a high concentration (100 µM) elicited cell death among the metabolites

examined (Fig. 2B, *inset*). Both M3 and M4 failed to induce the enzyme. In the subsequent

experiments, we chose the concentration of 30 µM to assess the effects of oltipraz's metabolites on the

gene expression.

Next, we examined the time-course effects of M1 and M2 on GSTA2 expression. Treatment of

cells with either M1 or M2 increased the levels of GSTA2 in a time-dependent manner (Fig. 3A and

3B). GSTA2 began to be induced 12 h after M1 or M2 treatment, and the enzyme induction was

sustained at 24 or 48 h (Fig. 3B). The extent of GSTA2 induction by M2 at 48 h, which was greater

than that by M1 at the same time point, was comparable to that by oltipraz. These results indicate that

either M1 or M2 induces GSTA2, whereas neither M3 nor M4 is active.

Effects of Oltipraz's Metabolites on C/EBPβ Activation. A previous study from this laboratory

has shown that oltipraz induces GSTA2 via C/EBPβ activation (Kang et al., 2003). We were interested

in whether GSTA2 induction by M1 or M2 depends on C/EBPβ, whose nuclear translocation activates

the C/EBP binding site present in the promoter region of the gene. Immunoblot analyses revealed that

the levels of C/EBPβ in the nuclear fractions were increased by M1 and to a lesser extent by M2 (Fig.

4A). Increase in nuclear C/EBPβ by M1 was almost equivalent to that by oltipraz. Neither M3 nor M4

stimulated nuclear accumulation of C/EBPβ (Fig. 4A, left). We also found that increase in the nuclear

C/EBPβ by M1 accompanied the increase in C/EBPβ expression in lysates (12 h)(Fig. 4A, right), as

was observed after oltipraz treatment (Lee and Kim, 2006). The induction of C/EBPβ by M2 was less

than that by M1. A time-course study showed that increases in nuclear C/EBPβ by M1 or M2 were

observed 12 h after treatment (Fig. 4B, left). Increase in the nuclear C/EBPβ by M1 was sustained up

to 24 h after treatment (Fig. 4B, right).

We further determined the effects of the metabolites on C/EBP DNA binding activity. Gel shift analysis of protein binding to the C/EBP binding site was performed with the nuclear extracts of cells treated with each metabolite (30 µM, 12 h) using a radiolabeled C/EBP binding oligonucleotide. Treatment of cells with M1 or oltipraz strongly increased the band intensity of C/EBP DNA binding compared to control (Fig. 4C, left). M2 treatment weakly enhanced the band intensity of C/EBP DNA binding, which was consistent with the result of immunoblot analysis. Immuno-inhibition experiments confirmed that C/EBP DNA binding activity in cells treated with M1 depended on C/EBPβ (Fig. 4C, right). Addition of a 20-fold excess of unlabeled C/EBP binding oligonucleotide, but not that of SP-1 binding oligonucleotide, to the nuclear extract abolished C/EBP binding to the C/EBP binding site. These data in conjunction with immunoblot results demonstrated that M1 activated C/EBPβ in H4IIE cells, as did oltipraz, and that C/EBPβ activation by M2 was much smaller than that by M1.

A supplemental RT-PCR assay revealed that C/EBPβ induction by M1 accompanied increases in its mRNA at 12-24 h (data not shown). In another study from this laboratory (Bae and Kim, 2005), an experiment using cycloheximide allowed us to find that oltipraz unaffected the half time of C/EBPβ protein. These results along with the fact that the promoter region of the *C/EBPβ* gene comprises C/EBPβ binding site (Lee and Kim, 2006) support the possibility that activating C/EBPβ induces its own gene in a transcriptional mechanism.

Role of C/EBP Activation for *GSTA2* Luciferase Induction. We next investigated whether the induction of GSTA2 by M1 or M2 was accompanied by *GSTA2* gene transactivation. Luciferase activity assays were performed in cells transfected with pGL-1651 which contained the luciferase gene downstream of the –1.65 kb *GSTA2* promoter region (Fig. 5, upper). Treatment of pGL-1651-transfected cells with M1 or M2 resulted in 3.6- or 4.0-fold increase in luciferase activity (Fig. 5, lower left). Transcription of the gene by M2 was as efficacious as that by oltipraz. As expected, neither M3 nor M4 increased luciferase activity.

To verify the functional role of the C/EBP response element in *GSTA2* gene induction by M1 or M2, we used pGL-1651-ΔC/EBP, in which the C/EBP binding site was specifically deleted by site-

directed mutagenesis. Luciferase-inducible activity by M1 or M2 was completely abolished in cells transfected with pGL-1651-ΔC/EBP (Fig. 5, lower right), compared with that in cells transfected with pGL-1651. These observations indicated that either M1 or M2 transactivated the *GSTA2* gene to a similar extent, as did oltipraz, and that *GSTA2* gene transactivation by the metabolites depended at least in part on C/EBPβ activation.

Role of ARE in *GSTA2* Luciferase Activity Induced by M2. Our result presented here showing that GSTA2 induction by M2 was not less than that by M1 despite its weak activation of C/EBPβ suggested that activation of other transcriptional factor by M2 may have contributed to the gene induction. Hence, we next examined the extents of Nrf2 activation by oltipraz's metabolites. Immunoblot analyses revealed that M2, but not M1, promoted Nrf2 accumulation in the nucleus (Fig. 6A). Either M3 or M4 was not active. Gel shift analysis confirmed that treatment of the cells with M2 (12 h) increased the binding activity of Nrf2 to the ARE, compared to control (Fig. 6B). M3 or M4 did not increase Nrf2 DNA binding. Competition experiments with anti-Nrf2 antibody or excess unlabeled oligonucleotide verified the specificity of Nrf2 DNA binding activity. Data supported the conclusion that only M2 among the metabolites examined was capable of activating Nrf2.

To assess the functional role of Nrf2 activation by M2 for ARE-driven *GSTA2* gene induction, we used pGL-1651-ΔARE, a chimeric gene construct with the ARE deleted (Fig. 6C, upper). Luciferase reporter gene analysis demonstrated that the ability of M2 to induce luciferase from pGL-1651 was abrogated by ARE deletion mutation (Fig. 6C, lower). The results presented here support the notion that Nrf2 activation by M2 contributes to the induction of *GSTA2* gene. The important consequence of this finding is that Nrf2, which serves as an active component in the ARE binding complex, is notably activated only by M2. Therefore, the greater GSTA2 induction by M2 than that by M1 may have resulted from its activation of Nrf2 as well as C/EBPβ.

Discussion

Oltipraz is an excellent candidate for cancer chemoprevention, which is considered to be mediated in part by the induction of GST detoxifying enzyme. We report here that M1, one of oltipraz's major metabolites, induces GSTA2, as does the parent compound. Both the relative potency and the efficacy of M1 in inducing GSTA2 were slightly smaller than those of oltipraz probably because of M1 being more hydrophilic. It is predicted that M2 is produced *in vivo* by a molecular rearrangement of oltipraz (Bieder et al., 1983; Fleury et al., 1985; Largeron et al., 1987). The time-course of GSTA2 induction by M2 at a concentration of 30 µM was comparable to that induced by oltipraz although M2 at a higher concentration (100 µM) was toxic to H4IIE cells. The lack of GSTA2 induction by M3 or M4, each of which is produced by oxidation of sulfide(s) in M2 to sulfone(s), suggested that the two sulfide moieties in M2 might have been responsible for the enzyme induction. Our finding presented here showing that conversion of sulfide(s) in M2 to sulfone(s) abrogated the abilities of M2 to induce cytotoxicity and to promote GSTA2 transactivation suggests that GSTA2 induction by M2 might be associated with the adaptive response against toxic insult.

Previously, we have shown that oltipraz promoted nuclear translocation of C/EBPβ and activated C/EBPβ binding to the target gene promoter, which led to the induction of GSTs (Kang et al., 2003). The putative C/EBPβ binding sites are found in the promoter regions of other phase II genes in mice or humans, which include human γ-glutamylcysteine synthetase, mouse quinone reductase, human GSTα and human hemeoxygenase-1 genes. Therefore, C/EBPβ may serve as a common transcriptional factor for the induction of phase II enzymes. In the present study, we found that M1, a 1,2-dithiole-3-one derivative, was capable of activating C/EBPβ, as observed after treatment with oltipraz, a 1,2-dithiole-3-thione derivative. The almost identical molecular structure of M1 to its parent compound with their possession of the common C/EBPβ-activating property renders us to conclude that GSTA2 induction by the agents might be mediated by the activation of C/EBPβ. The possibility that M1 may serve as a beneficial candidate for cancer chemoprevention is partly supported by the previous finding showing that M1 inhibited hepatic AFB1-DNA binding with the induction of multiple phase II enzymes *in vivo* (Kensler et al., 1987). The greater activation of C/EBPβ by M1 or oltipraz than that by M2 at the

respective same concentrations indicates that either the 1,2-dithiole-3-one or 1,2-dithiole-3-thione moiety has the sufficient ability to activate C/EBPβ. We found that M2 was also capable of promoting C/EBPβ activation, which was much smaller than that by M1 or its parent molecule. Furthermore, the mono- or di-sulfone derivative of M2 (M3, M4) failed to activate C/EBPβ. These observations further support the conclusion that the GSTA2-inducing ability of M1 or oltipraz, which has the 1,2-dithiole-3-one or 1,2-dithiole-3-thione moiety, results at least in part from C/EBPβ activation. The functional role of C/EBPβ in *GSTA2* gene induction was strengthened by the result of the luciferase reporter gene analysis using a mutant plasmid with the C/EBP-binding site being deleted.

The observation that the extent of GSTA2 induction by M2 was greater than that by M1 in spite of its weak C/EBPβ activation raised the possibility that activation of other transcriptional factor(s) might also contribute to the gene transactivation. Many of studies have shown that Nrf2 activation by oltipraz was responsible for the ARE-driven phase II enzyme induction (Iida et al., 2004; Ramos-Gomez et al., 2001). In the present study, M2 as one of the active metabolites of oltipraz strongly enhanced Nrf2 activation, as indicated by nuclear accumulation of Nrf2 and Nrf2's binding to ARE in the target gene promoter. Luciferase expression from the *GSTA2* gene as a consequence of Nrf2 activation by M2 depended on the ARE comprised in the gene, which was evidenced by ARE mutation analysis. Hence, it is highly likely that GSTA2 induction by M2 results from the activation of Nrf2 in combination with that of C/EBPβ. These results imply the possibility that Nrf2 activation by oltipraz might be due to M2 production from oltipraz. Our finding that M2 itself induces GSTA2 with Nrf2 activation is consistent with the previous report that the putative prodrug of M2 induces NQO1 (Petzer et al., 2003). In the study, one of M2 prodrugs was capable of stimulating Nrf2 activation and Nrf2-dependent luciferase expression in cells stably transfected with the ARE-3/luciferase gene comprising the luciferase gene preceded by three tandem copies of the mouse HO-1 ARE. It has been shown that the cytotoxic pro-oxidants such as diethylmaleate, S-(1,1,2,2-tetrafluoroethyl)-L-cysteine, *tert*-butylhydroquinone, paraquat and sodium arsenite induce phase II enzymes via strong Nrf2 activation (Kang et al., 2003; Ho et al., 2005; Ishii et al., 2000). Among the oxidized metabolites of oltipraz used in the present study, M2 was capable of activating Nrf2 with cell death induction at a high concentration. Based on the

15

results from this analysis, it can be speculated that Nrf2 activation by M2 may represent an adaptive response against the deleterious effect elicited by M2.

Nrf2 appeared to be an essential component for the induction of phase II detoxifying genes. Nrf2[(-/-)] mice developed a greater number of benzo[a]pyrene-initiated tumors than did the wild-type mice, providing evidence that oltipraz's chemoprotection against chemical-induced carcinogenesis requires Nrf2. Similarly, phase II enzyme induction by oltipraz requires the constitutive Nrf2 binding to the AREs located in the promoter regions of phase II detoxifying genes (Ramos-Gomez et al., 2001), being consistent with our earlier report showing that ARE deletion mutation prevented the *GSTA2* gene induction (Park et al., 2004; Kang et al., 2003). These findings are in line with the *in vivo* observation that the basal expression of phase II detoxifying genes was down-regulated by Nrf2 deficiency in animals (Enomoto et al., 2001), accompanying the loss of anticarcinogenic efficacy of oltipraz (Iida et al., 2004; Ramos-Gomez et al., 2001). This is reflected in part by our previous observations that both C/EBPβ and Nrf2 act together as transcription factors for the *GSTA2* gene (Park et al., 2004; Ki et al., 2005) and that activated C/EBPβ or Nrf2 interacts with CBP coactivator (Lee and Kim, 2006; Katoh et al., 2001). Therefore, M2 induces GSTA2 through Nrf2 activation, but requires the basal C/EBPβ binding to the C/EBP binding site for the gene induction. Similarly, the basal activation of ARE is necessary for C/EBPβ-mediated M1 induction of GSTA2. Hence, the constitutive bindings of both C/EBPβ and Nrf2 to their DNA elements render cooperative assembly of an activated transcription complex at the target gene. Although oltipraz is a potent inducer of phase II enzyme, inducible activation of Nrf2 by oltipraz seems to be not as strong as that of other pro-oxidants. Studies have shown that higher concentrations of oltipraz were required for Nrf2 activation and Nrf2 binding to the EpRE/ARE in HepG2 cells (Pietsch et al., 2003). Likewise, Nrf2 accumulation in the nuclear fraction had been observed in the livers of mice treated with as high as 500 mg/kg of oltipraz (Ramos-Gomez et al., 2001). Another study from this laboratory also showed that the mutant promoter, in which the C/EBP response element was deleted, was ineffective for *GSTA2* gene induction (Park et al., 2004). Hence, both C/EBPβ and Nrf2 act together as the constitutive and inducible transcription factors for the gene.

The estimated safe dosage level of oltipraz in the chronic toxicity studies was 10-30 mg/kg/day (Crowell et al., 1997). Oltipraz, originally studied as a schistosomicidal agent, has been applied to humans at a daily dose of 30 mg/kg (El et al., 1988). Oltipraz at 3-100 µM induced GSTA2 in H4IIE cells, and 30 µM of oltipraz was sufficient to almost maximally increase GSTA2 level (Kang et al., 2003), as confirmed by the present study. We have shown that the hepatic concentration of oltipraz 8 h after oral administration at a dose of 30 mg/kg to rats reached ~27 µM, which was 12 times of the plasma concentration (Bae et al., 2004). Hence, it is conceivable that the oltipraz concentrations achieved in the liver may be within the concentration range used in the present study. Our study presented here identifies the novel aspect that M2 at 100 µM induces cell death and at a lower concentration promotes nuclear translocation of Nrf2 and its DNA binding activity. The pharmacokinetic studies indicated that the C_{max} of M2 was not proportionally elevated by increasing doses of oltipraz at the range of 125-1000 mg/m^2 in humans (O'Dwyer et al., 2000). In their study, the C_{max} values of oltipraz were 1.5-3.0 µM, whereas those of M2 were 0.5-0.8 µM. It is predicted that the hepatic concentration of oltipraz may reach 18-36 µM at the 250-1000 mg/m^2 dose levels in humans. If oltipraz is metabolized into M2 in the human liver at the same rate as the rat, the hepatic concentration of M2 would reach 6.0-9.6 µM at the dose range. The pharmacokinetic study showed that the AUC and the C_{max} ratio of M2 to oltipraz were both limited as the metabolic conversion of oltipraz to M2 was saturated (O'Dwyer et al., 2000). Because the conversion ratio of oltipraz to M2 would be less than 0.3, M2 produced *in vivo* by the metabolism of a moderate dose of oltipraz may minimally contribute to the enzyme induction. By the same token, the level of M2 produced from oltipraz *in vivo* is unlikely to cause toxicity.

In conclusion, the present study provides evidence that M1 and M2 induce GSTA2, whereas M3 and M4 are inactive, and that M1 induces GSTA2 only via C/EBPβ activation, while M2 does so by activating Nrf2 as well as C/EBPβ (Fig. 7). These results substantiate the differential effects of oltipraz's metabolites on C/EBPβ- and/or Nrf2-mediated GSTA2 induction. The findings in this study led us to infer that Nrf2 activation by oltipraz in the previous literatures may result from M2, whose production is metabolically increased at high doses of oltipraz.

17

References

Bae EJ and Kim SG (2005) Enhanced CCAAT/enhancer-binding protein beta-liver-enriched inhibitory protein production by oltipraz, which accompanies CUG repeat-binding protein-1 (CUGBP1) RNA-binding protein activation, leads to inhibition of preadipocyte differentiation. *Mol Pharmacol* **68**:660-669.

Bae SK, Lee SJ, Lee JY, Lee Y, Lee I, Kim SG and Lee MG (2004) Pharmacokinetic changes of oltipraz after intravenous and oral administration to rats with liver cirrhosis induced by dimethylnitrosamine. *Int J Pharm* **275:**227-238.

Bieder A, Decouvelaere B, Gaillard C, Depaire H, Heusse D, Ledoux C, Lemar M, Le Roy JP, Raynaud L, Snozzi C and Gregoire J (1983) Comparison of the metabolism of oltipraz in the mouse, rat and monkey and in man. Distribution of the metabolites in each species. *Arzneimittelforschung* **33:**1289-1297.

Bolton MG, Munoz A, Jacobson LP, Groopman JD, Maxuitenko YY, Roebuck BD and Kensler TW (1993) Transient intervention with oltipraz against aflatoxin-induced hepatic tumorigenesis. *Cancer Res* **53:**3499-3504.

Corbet JP, Paris JM and Cotrel C (1982) Une Nouvelle reaction de cyclisation conduisant a des pyrrolo[1,2-a]pyrazines. *Tetrahedron Lett* **23:**3565-3566.

Curphey TJ (2000) A superior procedure for the conversion of 3-oxoesters to 3*H*-1,2-dithiole-3-thiones. *Tetrahedron Lett* **41:**9963-9966.

Curphey TJ (2002) Thionation of esters and lactones with the reagent combination of phosphorus pentasulfide and hexamethyldisiloxane. *Tetrahedron Lett* **43:**371-373.

Curphey TJ and Libbyt AH (2000) Dianions of 3-oxodithioic acids: preparation and conversion to 3*H*-1,2-dithiole-3-thiones. *Tetrahedron Lett* **41:**6977-6980.

El Tayeb M, Daffalla AA, Kardaman MW, See R. and Fenwick A. (1988) Praziquantel and oltipraz: the treatment of schoolchildren infected with *Schistosoma mansoni* and/or *Schistosoma haematobium* in Gezira, Sudan. *Ann Trop Med Parasitol* **82:**53-57.

Enomoto A, Itoh K, Nagayoshi E, Haruta J, Kimura T, O'Connor T, Harada T and Yamamoto M (2001) High sensitivity of Nrf2 knockout mice to acetaminophen hepatotoxicity associated with decreased

expression of ARE-regulated drug metabolizing enzymes and antioxidant genes. *Toxicol Sci* 5**9:**169-177.

Fleury MB, Largeron M, Barreau M and Vuilhorgne M (1985) Studies of the reaction of 1,2-dithiole-thiones with nucleophiles. *Tetrahedron* **41:**3705-3715.

Ho HK, White CC, Fernandez C, Fausto N, Kavanagh TJ, Nelson SD and Bruschi SA (2005) Nrf2 activation involves an oxidative-stress independent pathway in tetrafluoroethylcysteine-induced cytotoxicity. *Toxicol Sci* **86:**354-364.

Huang HC, Nguyen T and Pickett CB (2000) Regulation of the antioxidant response element by protein kinase C-mediated phosphorylation of NF-E2-related factor 2. *Proc Natl Acad Sci USA* **97:**12475-12480.

Iida K, Itoh K, Kumagai Y, Oyasu R, Hattori K, Kawai K, Shimazui T, Akaza H and Yamamoto M. (2004) Nrf2 is essential for the chemopreventive efficacy of oltipraz against urinary bladder carcinogenesis. *Cancer Res* **64:**6424-6431.

Ishii T, Itoh K, Takahashi S, Sato H, Yanagawa T, Katoh Y, Bannai S and Yamamoto M (2000) Transcription factor Nrf2 coordinately regulates a group of oxidative stress-inducible genes in macrophages. *J Biol Chem* **275:**16023-16029.

Jackson PE and Groopman JD (1999) Aflatoxin and liver cancer. *Baillieres Best Pract Res Clin Gastroenterol* **13:**545-555.

Jacobson LP, Zhang BC, Zhu YR, Wang JB, Wu Y, Zhang QN, Yu LY, Qian GS, Kuang SY, Li YF, Fang X, Zarba A, Chen B, Enger C, Davidson NE, Gorman MB, Gordon GB, Prochaska HJ, Egner PA, Groopman JD, Munoz A, Helzlsouer KJ and Kensler TW (1997) Oltipraz chemoprevention trial in Qidong, People's Republic of China: study design and clinical outcomes. *Cancer Epidemiol Biomarkers Prev* **6:**257-265.

Jaitovitch-Groisman I, Fotouhi-Ardakani N, Schecter RL, Woo A, Alaoui-Jamali MA and Batist G (2000) Modulation of glutathione S-transferase alpha by hepatitis B virus and the chemopreventive drug oltipraz. *J Biol Chem* **275:**33395-33403.

Kang KW, Cho IJ, Lee CH and Kim SG. (2003) Essential role of phosphatidylinositol 3-kinase-dependent CCAAT/enhancer binding protein-β activation in the induction of glutathione S-

transferase by oltipraz. *J Natl Cancer Inst* **95:**53-66.

Katoh Y, Itoh K, Yoshida E, Miyagishi M, Fukamizu A, and Yamamoto M (2001) Two domains of Nrf2 cooperatively bind CBP, a CREB binding protein, and synergistically activate transcription. *Genes Cells* **6**:857-868.

Kensler TW, Egner PA, Dolan PM, Groopman JD and Roebuck BD (1987) Mechanism of protection against aflatoxin tumorigenicity in rats fed 5-(2-pyrazinyl)-4-methyl-1,2-dithiol-3-thione (oltipraz) and related 1,2-dithiol-3-thiones and 1,2-dithiol-3-ones. *Cancer Res* **47:**4271-4277.

Kensler TW (1997) Chmoprevention by inducers of carcinogen detoxication enzymes. *Environ Health Perspect* 105**:**965-970.

Ki SH, Cho IJ, Choi DW and Kim SG (2005) Glucocorticoid receptor (GR)-associated SMRT binding to C/EBPβ TAD and Nrf2 Neh4/5: role of SMRT recruited to GR in GSTA2 gene repression. *Mol Cell Biol* **25:**4150-4165.

Kwak MK, Egner PA, Dolan PM, Ramos-Gomez M, Groopman JD, Itoh K, Yamamoto M and Kensler TW (2001) Role of phase 2 enzyme induction in chemoprotection by dithiolethiones. *Mutat Res* 480**:**305-315.

Largeron M, Martens T and Fleury MB (1987) Reactivity of substituted 1,2-dithiole-3-thiones with sodium ethanethiolate: a convenient route to a novel heterocycle. *Tetrahedron Lett* **43:**3421-3428.

Lee SJ and Kim SG (2006) Role of RSK1 in oltipraz-induced specific phosphorylation of C/EBPβ for GSTA2 gene transactivation. *Mol Pharmacol* **69:**385-396.

Moinova HR and Mulcahy RT (1998) An electrophile responsive element (EpRE) regulates beta-naphthoflavone induction of the human gamma-glutamylcysteine synthetase regulatory subunit gene. Constitutive expression is mediated by an adjacent AP-1 site. *J Biol Chem* **273:**14683-14689.

Nelson KC, Armstrong JS, Moriarty S, Cai J, Wu MV, Sternberg P Jr and Jones DP (2002) Protection of retinal pigment epithelial cells from oxidative damage by oltipraz, a cancer chemopreventive agent. *Investig Ophthalmol Vis Sci* **43:**3550-3354.

O'Dwyer PJ, Clayton M, Halbherr T, Myers CB and Yao K (1997) Cellular kinetics of induction by oltipraz and its keto derivative of detoxication enzymes in human colon adenocarcinoma cells. *Clin Cancer Res* **3:**783-791.

O'Dwyer PJ, Szarka C, Brennan JM, Laub PB and Gallo JM (2000) Pharmacokinetics of the chemopreventive agent oltipraz and of its metabolite M3 in human subjects after a single oral dose. *Clin Cancer Res* **6:**4692-4696.

Park EY, Cho IJ and Kim SG (2004) Transactivation of the PPAR-responsive enhancer module in chemopreventive glutathione S-transferase gene by the peroxisome proliferator-activated receptor-γ and retinoid X receptor heterodimer. *Cancer Res* **64:**3701-3713.

Petzer JP, Navamal M, Johnson JK, Kwak MK, Kensler TW and Fishbein JC (2003) Phase 2 enzyme induction by the major metabolite of oltipraz. *Chem Res Toxicol* **16:**1463-1469.

Pietsch EC, Chan JY, Torti FM and Torti SV (2003) Nrf2 mediates the induction of ferritin H in response to xenobiotics and cancer chemopreventive dithiolethiones. *J Biol Chem* **278:**2361-2369.

Ramos-Gomez M, Kwak MK, Dolan PM, Itoh K, Yamamoto M, Talalay P and Kensler TW (2001) Sensitivity to carcinogenesis is increased and chemoprotective efficacy of enzyme inducers is lost in *nrf2* transcription factor-deficient mice. *Proc Natl Acad Sci USA* **98:**3410-3415.

Rao CV, Rivenson A, Katiwalla M, Kelloff GJ and Reddy BS (1993) Chemopreventive effect of oltipraz during different stages of experimental colon carcinogenesis induced by azoxymethane in male F344 rats. *Cancer Res* **53:**2502-2506.

Venugopal R and Jaiswal AK (1998) Nrf2 and Nrf1 in association with Jun proteins regulate antioxidant response element-mediated expression and coordinated induction of genes encoding detoxifying enzymes. *Oncogene* **17:**3145-3156.

Wang JS, Shen X, He X, Zhu YR, Zhang BC, Wang JB, Qian GS, Kuang SY, Zarba A, Egner PA, Jacobson LP, Munoz A, Helzlsouer KJ, Groopman JD and Kensler TW (1999) Protective alterations in phase 1 and 2 metabolism of aflatoxin B1 by oltipraz in residents of Qidong, People's Republic of China. *J Natl Cancer Inst* **91:**347-354.

DMD #9514

Footnotes

Legends for Figures

Fig. 1. The chemical structures of oltipraz and its major metabolites.

Fig. 2. The concentration-response effects of oltipraz and metabolites on the expression of GSTA2.
A) Immunoblot analysis of GSTA2. GSTA2 was immunoblotted in the lysates prepared from H4IIE
cells treated with oltipraz, M1, M2, M3 or M4 at the concentrations of 10-100 µM for 24 h. Each lane
was loaded with 10 µg of lysate proteins. Immunoreactive GSTA2 was visualized by horseradish
peroxidase-conjugated secondary antibody and an enhanced chemiluminescence detection kit. Equal
loading of proteins was verified by probing the replicate blots for actin. **B)** The relative GSTA2 levels.
Changes in GSTA2 relative to untreated control were assessed by scanning densitometry of the
immunoblots. Data represent the mean±S.E. with 3 separate experiments (significant compared to
control, *$p<0.05$, **$p<0.01$; untreated control = 1). *Inset* shows the effect of M2 on the viability of
H4IIE cells. Cells were incubated in the medium containing 10-100 µM M2 for 24 h and the viability
of the cells was assessed by MTT assay. Data represent the mean±S.E. with 8 separate experiments
(significant compared to control, **$p<0.01$).

Fig. 3. The time-course effects of oltipraz, M1 and M2 on the expression of GSTA2. **A)** Immunoblot
analysis of GSTA2. GSTA2 was immunoblotted in the lysates prepared from cells treated with oltipraz,
M1 or M2 at a concentration of 30 µM for 12-48 h. Each lane was loaded with 10 µg of proteins.
Equal loading of proteins was verified by probing the replicate blots for actin. **B)** The relative GSTA2
levels. The protein levels were assessed by scanning densitometry of the immunoblots. Data represent
the mean±S.E. with 3 separate experiments (significant compared to control, *$p<0.05$, **$p<0.01$;
control = 1).

Fig. 4. The effects of oltipraz and its metabolites on the activation of C/EBPβ. **A)** Immunoblot analysis

of C/EBPβ. C/EBPβ was immunoblotted in the nuclear or lysate fractions of H4IIE cells treated with oltipraz or its metabolite. Equal loading of proteins was verified by actin immunoblotting. **B)** The time-course effects of oltipraz, M1 and M2 on the levels of nuclear C/EBPβ. C/EBPβ was immunoblotted in the nuclear fractions of cells treated with oltipraz, M1 or M2 for the indicated time period. Equal loading of proteins was verified by actin immunoblotting. **C)** Gel shift analysis of C/EBP DNA binding. Gel shift analysis was performed with a radiolabeled C/EBP binding oligonucleotide and the nuclear fractions prepared from cells treated with oltipraz or metabolite. An arrowhead indicates the DNA bound with C/EBPβ (left). Immuno-competition analyses were carried out by incubating the nuclear extract of M1-treated cells (30 µM, 12 h) with the specific polyclonal antibody directed against C/EBPβ or C/EBPα (2 µg each) for 1 h. For competition assays, a 20-fold molar excess of unlabeled C/EBP or SP-1 binding oligonucleotide was added to the nuclear extract (right).

Fig. 5. The role of C/EBP activation by oltipraz and its metabolites for *GSTA2* gene induction. A scheme shows the C/EBP binding site and ARE in pGL-1651 that contains the promoter region of the *GSTA2* gene and the coding region of luciferase. pGL-1651-ΔC/EBP represents a mutant construct of pGL-1651, in which the C/EBP binding site was specifically deleted. The cells transfected with pGL-1651 (or pGL-1651-ΔC/EBP) and CMV-β-galactosidase plasmid (33:1) were exposed to oltipraz or metabolite (30 µM, 24 h). The luciferase reporter gene activity was calculated as a relative change to that of β-galactosidase. The value represented the mean±S.E. with 4 separate experiments (significant compared to control, **$p<0.01$; significant compared to pGL-1651-transfected cells treated with M1 or M2, [##]$p<0.01$; control = 1).

Fig. 6. The effects of oltipraz's metabolites on Nrf2 activation. **A)** Immunoblot analysis of nuclear Nrf2. Nrf2 was immunoblotted in the nuclear fractions of H4IIE cells treated with M1, M2, M3 or M4. Equal loading of proteins was verified by actin immunoblotting. **B)** Gel shift analysis of Nrf2 DNA

binding. Gel shift analysis was performed with a radiolabeled ARE and nuclear proteins prepared from cells treated with each metabolite. An arrowhead indicates the ARE bound with Nrf2 (left). Immunocompetition assay of Nrf2 binding to ARE was performed with anti-Nrf2 antibody (2 μg, 1 h). A 20-fold molar excess of unlabeled SP-1 or ARE binding oligonucleotide was added to the nuclear extract of M2-treated cells (30 μM, 12 h) for competition assays (right). **C)** The effect of M2 on the induction of luciferase activity from pGL-1651 or pGL-1651-ΔARE. Luciferase activity was measured in cells transfected with pGL-1651 or pGL-1651-ΔARE, as described in Fig. 5, and subsequently exposed to vehicle or M2. The value represented the mean±S.E with 4 separate experiments (significant compared to control, **$p<0.01$; significant compared to pGL-1651-transfected cells treated with M2, ##$p<0.01$; control = 1).

Fig. 7. A schematic diagram illustrating the proposed mechanism, by which oltipraz and its major metabolites differentially transactivate the *GSTA2* gene. Oltipraz is biotransformed to M1 or M2. M2 is further metabolized to M3 or M4. M1 promotes C/EBPβ activation, whereas M2 activates Nrf2 as well as C/EBPβ for the gene induction.
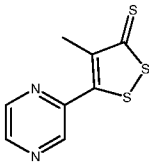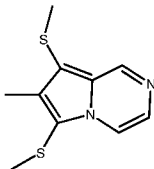
4-methyl-5-(2-pyrazinyl)-1,2-dithiol-3-thione
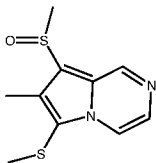
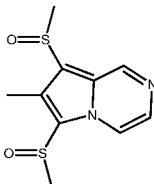(Oltipraz)
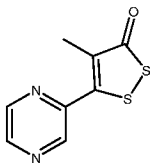
4-methyl-5-(pyrazin-2-yl)-3H-1,2-dithiol-3-one

(M1)

7-methyl-6,8-bis(methylthio)H-pyrrolo-[1,2-a]pyrazine

(M2)

7-methyl-8-(methylsulfinyl)-
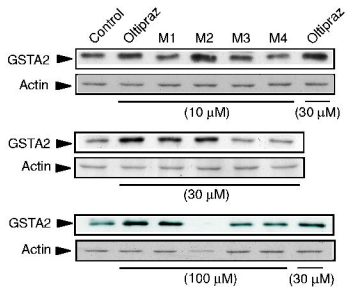6-(methylthio)H-pyrrolo[1,2-a]pyrazine

(M3)

7-methyl-6,8-bis(methylsulfinyl)H-
pyrrolo[1,2-a]pyrazine

(M4)

Fig. 1

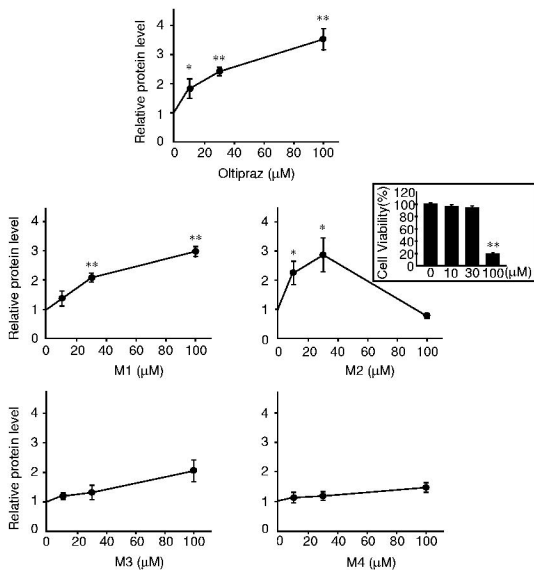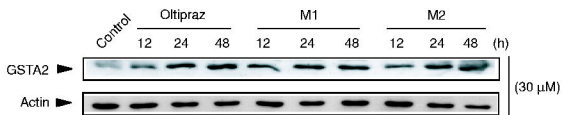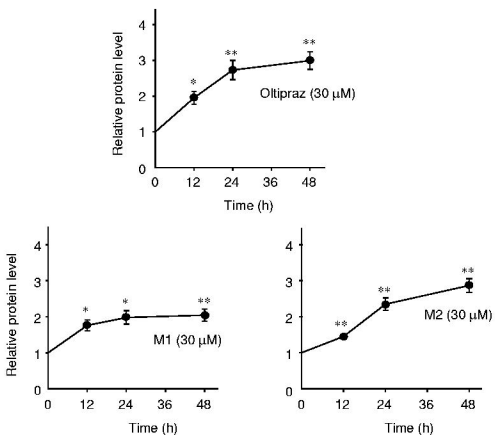A)

GSTA2

Actin

Control Oltipraz M1 M2 M3 M4 Oltipraz

(10 μM) (30 μM)

GSTA2

Actin

(30 μM)

GSTA2

Actin

(100 μM) (30 μM)

B)

Fig. 2

A)

	Control	Oltipraz			M1			M2		
		12	24	48	12	24	48	12	24	48 (h)

GSTA2 ▶

Actin ▶

(30 μM)

B)

Oltipraz (30 μM)

M1 (30 μM)

M2 (30 μM)

Fig. 3

A)

Nuclear fraction | Lysate

Control Oltipraz M1 M2 M3 M4 | Control Oltipraz M1 M2

C/EBPβ ►

Actin ►

(30 μM, 12 h)

B)

Control Oltipraz (12h) | M1 3 6 12 | M2 3 6 12 (h) | Control | M1 12 24 48 (h)

Nuclear C/EBPβ ►

Actin ►

(30 μM)

C)

(30 μM, 12 h)

Control Oltipraz M1 M2 M3 M4 | Control M1 +Anti-C/EBPβ Ab +Anti-C/EBPα Ab | M1 +C/EBP (20X) +SP-1 (20X)

DNA bound with C/EBP ►

Fig. 4

Fig. 5

A)

Nuclear Nrf2

Actin

(30 μM, 12 h)

Control M1 M2 M3 M4

B)

(30 μM, 12 h)

Control M1 M2 M3 M4

DNA bound
with ARE

Control M2 + Anti-Nrf2 Ab

M2 + SP-1 (20X) + ARE (20X)

C)

Luciferase

|C/EBP| |ARE| pGL-1651
-1651   -905   -696

Luciferase

|C/EBP| pGL-1651-ΔARE
-1651   -905   -696

Relative luciferase activity

**

##

Control M2   Control M2   (30 μM, 24 h)
pGL-1651   pGL-1651-ΔARE

Fig. 6

Plasma membrane

Oltipraz → rearrangement → M2 → oxidation → M3 → oxidation → M4

oxidation → M1

C/EBPβ

Nrf2

Nucleus

C/EBPβ

C/EBP-RE

Nrf2 — Maf

ARE

GSTA2 gene transcription

Fig. 7